

Characterizing the Peak in the Cosmic Microwave Background Angular Power Spectrum

Lloyd Knox¹ and Lyman Page²

¹*Department of Astronomy and Astrophysics, University of Chicago, 5640 South Ellis Avenue, Chicago, Illinois 60637*

²*Department of Physics, Princeton University, Princeton, New Jersey*

(Received 9 February 2000; revised manuscript received 8 May 2000)

A peak has been unambiguously detected in the cosmic microwave background angular spectrum. Here we characterize its properties with fits to phenomenological models. We find that the TOCO and BOOM/NA data determine the peak location to be in the range 175–243 and 151–259, respectively (at 95% confidence) and determine the peak amplitude to be between ≈ 70 and $90 \mu\text{K}$. The peak shape is consistent with inflation-inspired flat, cold dark matter plus cosmological constant models of structure formation with adiabatic, nearly scale invariant initial conditions. It is inconsistent with open models and presents a great challenge to defect models.

PACS numbers: 98.70.Vc, 98.80.Cq

Introduction.—If the adiabatic cold dark matter (CDM) models with scale-invariant initial conditions describe our cosmogony, then an analysis of the anisotropy in the cosmic microwave background (CMB) can reveal the cosmological parameters to unprecedented accuracy [1]. A number of studies have aimed at determining, with various prior assumptions, a subset of the ~ 10 free parameters that affect the statistical properties of the CMB [2,3]. The parameter most robustly determined from current data is Ω , the ratio of the mean matter/energy density to the critical density (that for which the mean spatial curvature is zero). These investigations show that Ω is close to one. This result, combined with other cosmological data, implies the existence of some smoothly distributed energy component with negative pressure such as a cosmological constant.

A weakness of previous approaches [2,3] is that the conclusions depend on the validity of the assumed model. In this Letter we take a different tack and ask what we know independent of the details of the cosmological model [4]. We find the peak location, amplitude, and width are consistent with those expected in adiabatic CDM models. Furthermore, as $l_{\text{peak}} \approx 200 \Omega^{-1/2}$ in these models, the observed peak location implies $\Omega \approx 1$. The determination of the peak location is robust; it does not depend on the parametrization of the spectrum, assumptions about the distribution of the power spectrum measurement errors, nor on the validity of any one data set. The model-dependent determinations of Ω are further supported by the *inconsistency* of the data with competing models, such as topological defects, open models with $\Omega < 0.4$, or the simplest isocurvature models.

The data.—The year 1999 saw new results from MSAM [5], PythonV [6], MAT/TOCO [7,8], Viper [9], CAT [10], IAC [11], and BOOM/NA [12], all of which have bearing on the properties of the peak. These results are plotted in Fig. 1. We have known for several years that there is a rise towards $l = 200$. Now we see that there is also a significant drop towards $l = 400$.

For all the medium angular scale experiments, the largest systematic effect is the calibration error which is

roughly 10% for each. Contamination from foreground emission is also important and not yet fully accounted for in some experiments (e.g., TOCO). A correction for this contribution, for which $\delta T_l \sim l^{-1/2}$, will affect the amplitude of the peak, though it will not strongly affect its position. Thorough analyses by the MSAM [13] and

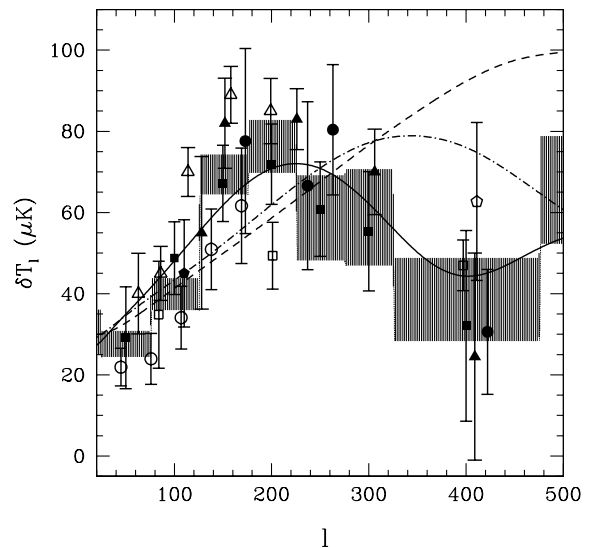


FIG. 1. Band powers from TOCO97 (open triangles), TOCO98 (filled triangles), BOOM/NA (filled squares), MSAM (open squares), CAT (black open pentagon), IAC (filled pentagon), PyV (black open circles), and Viper (filled circles). The y axis is $\delta T_l \equiv \sqrt{l(l+1)C_l/(2\pi)}$ where C_l is the angular spectrum. The models are, peaking at left to right, the best fit models of [3] for $\Omega = 1$, $\Omega = 0.4$, and $\Omega = 0.2$. The $\Omega = 1$ model has a mean density of nonrelativistic matter, $\Omega_m = 0.31$, a cosmological constant density of $\Omega_\Lambda = 0.69$, a baryon density of $\Omega_b = 0.019h^{-2}$ [15], a Hubble constant of $H_0 = 65 \text{ km/sec Mpc}$, an optical depth to reionization of $\tau = 0.17$, and a power spectrum power-law index of $n = 1.12$, where $n = 1$ is scale invariant. The shaded areas are the results of fitting the power in 14 bands of l to all the data (from 1999 and previous years) as in [16]. Many of the bands are at low l and cannot be discerned on this plot. Calibration errors are not shown, though they are included in the best fit.

PYTHON [6] teams show that the level of foreground contamination in those experiments is $<3\%$.

The three experiments that have taken data that span the peak are MSAM, TOCO, and BOOM/NA. All experiments exhibit a definite increase over the Sachs-Wolfe plateau though the significance of a feature based on the data alone, e.g., a peak, differs between experiments. We may assess the detection of a feature by examining the deviation from the best fit flat line, $\overline{\delta T}$. For the three MSAM points, we find $\overline{\delta T} = 46 \pm 4.9 \mu\text{K}$ (calibration error not included) with a reduced χ^2 of 0.43 (probability to exceed, $P_{>\chi^2} = 0.65$). Thus, no feature is detected with these data alone though there is a clear increase over DMR [14]. For the seven BOOM/NA points, we find $\overline{\delta T} = 55.3 \pm 4.2 \mu\text{K}$ with a reduced χ^2 of 1.94 ($P_{>\chi^2} = 0.05$, assuming the data are anticorrelated at the 0.1 level [12]). For the ten TOCO points, $\overline{\delta T} = 69.3 \pm 2.7 \mu\text{K}$ with a reduced χ^2 of 4.86 ($P_{>\chi^2} < 10^{-5}$). Calibration errors will not change χ^2/ν , though a correction for foreground emission will have a slight effect. We examine all data in the following, but we focus particularly on BOOM/NA and TOCO because of their detections of a feature.

Fits to phenomenological models.—To characterize the peak amplitude and location we fit the parameters of five different phenomenological models. For the first, we start with the best fit DK99 [3] adiabatic CDM model, δT_l^{DK} , and form $\delta T_l = \alpha(\delta T_l^{DK} - \delta T_{l=10}^{DK}) + \delta T_{l=10}^{DK}$ by varying α , and then stretching in l . We characterize each stretching with the peak position and peak amplitude. This method has the virtue that the resulting spectra resemble adiabatic models and so if one assumes that these models describe Nature, then these results are the ones to which we should pay the most attention.

Our second model for δT_l^2 is a Gaussian: $\delta T_l^2 = A^2 \exp[-(l - l_c)^2/(2\sigma_l^2)]$. Depending on the width, this spectrum can look very much like, or unlike, the spectra of adiabatic models [17]. We view this versatility as a virtue since we are interested in a characterization of the peak which is independent of physical models.

Finally, we also determined the peak location and amplitude with a damped sinusoid [$\delta T_l^2 = B + A^2 \exp(-l/l_c) \sin^2(2\pi l/l_x)$] with B set to agree with DMR, a pulse function, and an interpolation of the DK models (with an extrapolation to smaller l_{peak} values by steady increases in Ω_Λ from the DK best-fit flat model, sending $\Omega > 1$).

We fit to these phenomenological models in two ways. For the stretch model, we examine the χ^2 of the residuals between the published data and each model. The widths of the window functions are ignored and we assume the data are normally distributed in δT_l with a dispersion given by the average of the published error bars (GT in Table I). This is an admittedly crude method, but it works well because the likelihoods as a function of δT_l are moderately well approximated by normal distributions.

For both the Gaussian shape and the stretch model, we also perform the full fit as outlined in BJK [16] (Rad in Table I). For the Gaussian shape model, the constraints on the amplitude and location are given below after marginalization over the width σ_l . In all fitting, we ignore the experiments that are affected by $l < 30$ because we want the parameters of our Gaussian to be determined by behavior in the peak region.

The main thing to notice in Table I is that the position of the peak is robustly determined by *either* TOCO or BOOM/NA to be in the range 185 to 235, regardless of the method. Also see Fig. 2. For the quoted errors,

TABLE I. Details of the fits. All stands for all publically available data sets (except for VIPER which was not used because of unspecified point-to-point correlations), the T is for the TOCO data, the B for BOOM/NA and the P is for “Previous,” meaning all data prior to BOOM/NA and TOCO. G, S, Pu, DS, and DK are for the Gaussian shape, stretch, pulse, damped sinusoid, and DK methods, respectively. The DS result here is for $l_c = 500$; $l_c = 250$ and $l_c = 1000$ gave similar results. N is the number of data points and ν the degrees of freedom. Rad₀ and Rad_∞ correspond to log normal and normal distributions for the likelihood, respectively.

Data	Model	Fit	N/ν	χ^2/ν	$P_{>\chi^2}$	l_{peak}	δT_{peak} μK
All	G	Rad	58/55	1.25	0.10	229 ± 8.5	78
All	DK	Rad	58/56	1.16	0.19	220 ± 8.0	75
T	G	Rad	10/7	0.41	0.89	206 ± 16	95 ± 9
T	S	GT	10/8	0.94	0.48	214 ± 14	88 ± 9
T	Pu	Rad	10/7	1.0	0.43	211 ± 17	88 ± 9
T	DS	Rad	10/8	1.1	0.35	216 ± 18	88 ± 8
B	G	Rad _∞	7/4	0.19	0.94	208 ± 21	69 ± 9
B	S	GT	7/5	0.39	0.85	215 ± 24	69 ± 8
B	S	Rad ₀	7/5	0.23	0.95	205 ± 27	72 ± 8
B	S	Rad _∞	7/5	0.39	0.85	206 ± 26	68 ± 8
B	Pu	Rad _∞	7/5	1.0	0.41	210 ± 24	64 ± 8
B	DS	Rad _∞	7/4	0.46	0.81	207 ± 25	66 ± 8
P	G	Rad	33/30	1.13	0.28	262 ± 24	68
T98	S	Rad	5/3	0.86	0.46	212 ± 27	89 ± 10

we have marginalized over all parameters except the position. The peak amplitudes are subject to change as there is some dependence on the model parametrization and the foreground contamination has not been accounted for.

We account for the calibration uncertainty through a convolution of the likelihood of the fits with a normal distribution of the fractional error [16,18]. BOOM/NA, TOCO97 and TOCO98 have calibration uncertainties of 8%, 10.5%, and 8%, respectively. However, 5% of this is due to uncertainty in the temperature of Jupiter and therefore, common to all experiments. By comparing a simplified likelihood with one effective calibration, to a determination of the full likelihood that properly treats the common and uncommon contributions to calibration uncertainty, we attribute an effective calibration error of 8.5% to the TOCO data.

For the Gaussian model we can also marginalize over A and l_c to place 95% confidence bounds on the width: $75 < \sigma_l < 105$ for All, $50 < \sigma_l < 105$ for TOCO, and $55 < \sigma_l < 145$ for BOOM/NA.

Are the data in Fig. 1 consistent? DK99 found that the best-fit model, given all the data at the time, had a χ^2 of 79 for 63 degrees of freedom, which is exceeded 8% of the time. Here we see that the χ^2 for the fit of the Gaussian model is 69 for 55 degrees of freedom, which is exceeded 10% of the time. We conclude that, although there may well be systematic error in some of these data sets, we have no compelling evidence of it. However, we take caution from the fact that we had to adjust the calibration parameters from their nominal values to their best-fit values in order to reduce the χ^2 to 69. Left at their nominal values with calibration uncertainty ignored, the data are not consistent with each other. Thus we believe that the compilation results are perhaps less reliable than those for either BOOM/NA or TOCO. We do not quote their amplitude uncertainties in the table, and urge the reader not to over interpret their l_{peak} determinations.

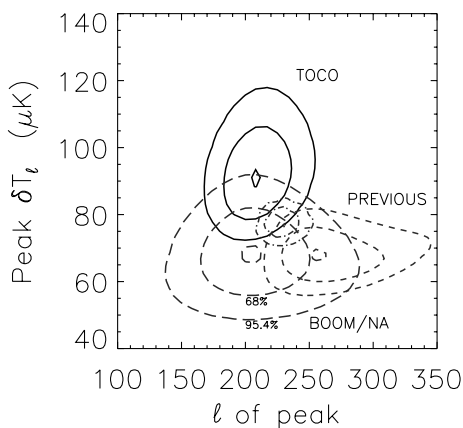


FIG. 2. Likelihood contours for l vs δT_l for the position of the peak. For BOOM/NA and TOCO, we use the stretch method using RADPACK [19] and include the calibration error. For Previous and All (tightest contours) we have fixed the calibration parameters. All contour levels correspond to 5%, 68%, and 95% enclosed, or roughly the peak, 1σ , 2σ .

Despite our attempt to provide an analysis independent of any physical models, we have assumed Gaussianity. Note, however, that there is no evidence for departures from Gaussianity strong enough to alter our results [20]. And further, if the CMB were strongly non-Gaussian, then we would expect to find bad χ^2 values even after adjustment of calibration uncertainty.

Implications for physical models.—Flat, adiabatic, nearly scale-invariant models have similar peak properties to those of our best-fit phenomenological models. Most importantly, the peak location, as determined by three independent data sets (“Previous,” TOCO, BOOM/NA), is near $l \simeq 210$, as expected. Depending on the data set chosen, the amplitude is higher than expected but can easily be accommodated, within the uncertainties, with a cosmological constant.

A good approximation to the first peak in the DK99 best-fit model is given by the Gaussian model with $\sigma_l = 95$. From the σ_l constraints quoted earlier we see that the data have no significant preference for peaks that are either narrower or broader than those in inflation-inspired CDM models.

A general perturbation is a combination of adiabatic and isocurvature perturbations. Adiabatic perturbations are such that at each point in space, the fractional fluctuations in the number density of each particle species is the same for all species. Isocurvature perturbations are initially arranged so that, despite fluctuations in individual species, the total energy density fluctuation is zero. Given multiple components, there are a number of different ways of maintaining the isocurvature condition. Below we assume the isocurvature condition is maintained by the dark matter compensating everything else.

Isocurvature initial conditions result in shifts to the CMB power spectrum peak locations. For a given wave number, the temporal phase of oscillations in the baryon-photon fluid depends on the initial relation between the dark matter and the fluid. Those waves with oscillation frequencies such that they hit an extremum at the time of last scattering in the adiabatic case, will hit a null in the isocurvature case [21]. The effect on the first (prominent) peak is a shift to higher l .

However, the observation of a peak near $l \sim 210$ cannot in itself rule out these isocurvature models, because the peak can be shifted back by taking $\Omega > 1$. Rather, these models are ruled out by the observed amplitude of the peak relative to the Sachs-Wolfe (SW) plateau; the SW plateau is a factor of 6 times larger than in the adiabatic case. To rectify this situation a large blue tilt would be required with a break at comoving length scales shorter than ~ 100 Mpc to avoid violating constraints on fluctuations on the $8h^{-1}$ Mpc scale [22].

Critical to the Doppler peak structure, in either adiabatic or isocurvature models, is the temporal phase coherence for Fourier modes of a given wave number [23]. In topological defect models, the continual generation of new perturbations by the nonlinear evolution of the defect

network destroys this temporal phase coherence and the acoustic peaks blend into a broad hump which is wider and peaks at higher l than the observed feature.

One can make defect model power spectra with less power at $l = 400$ than at $l = 200$ with *ad hoc* modifications to the standard ionization history [24]. But even for these models the drop is probably not fast enough [25]. The contrast between the power at $l = 200$ and $l = 400$ is a great challenge for these models.

There are scenarios with initially isocurvature conditions that can produce CMB power spectra that look much like those in the adiabatic case. This can be done by adding to the adiabatic fluctuations (of photons, neutrinos, baryons, and cold dark matter) another component, with a nontrivial stress history, which maintains the isocurvature condition [26].

Conclusions.—Our phenomenological models have allowed for rapid, model-independent, investigation of the consistency of CMB datasets, and of the robustness of the properties of the peak in the CMB power spectrum. The peak has been observed by two different instruments, and can be inferred from an independent compilation of other data sets. The properties of this peak are consistent with those of the first peak in the inflation-inspired adiabatic CDM models, and inconsistent with a number of competing models. It is perhaps instructive that where the confrontation between theory and observation can be done with a minimum of theoretical uncertainty, the adiabatic CDM models have been highly successful.

L. K. thanks A. Albrecht, S. Meyer, and M. Tegmark for useful conversations and is supported by the DOE, NASA Grant No. NAG5-7986 and NSF Grant No. OPP-8920223. L. P. thanks TOCO team members Mark Devlin, Randy Dorwart, Rob Caldwell, Tom Herbig, Amber Miller, Michael Nolta, Jason Puchalla, Eric Torbet, and Huan Tran, for insights and encouragement; and Chuck Bennett and Barth Netterfield for discussions and comments on earlier versions of this work. L. P. is supported by NSF Grant No. PHY96-00015 and NASA Grant No. NAS5-96021. During the review process, new BOOMERANG data were published [27]. They found $l_{\text{peak}} = 197 \pm 6$ and $\delta T_{\text{peak}} = 69 \pm 9 \mu\text{K}$, in agreement with our results here.

-
- [1] For example, L. Knox, Phys. Rev. D **52**, 4307 (1995); G. Jungman, M. Kamionkowski, A. Kosowsky, and D. N. Spergel, Phys. Rev. Lett. **76**, 1007 (1996); Phys. Rev. D **54**, 1332 (1996); J. R. Bond, G. Efstathiou, and M. Tegmark, Mon. Not. R. Astron. Soc. **33**, 291L (1997); M. Zaldarriaga, D. Spergel, and U. Seljak, Astrophys. J. **488**, 1 (1997); D. Eisenstein, W. Hu, and M. Tegmark, Astrophys. J. **518**, 2 (1999).
- [2] M. Tegmark and M. Zaldarriaga, astro-ph/0002091; A. Melchiorri *et al.*, astro-ph/9911445; N. Bahcall, J. P. Ostriker, S. Perlmutter, and P. J. Steinhardt, Science **284**, 1481

- (1999); J. G. Bartlett, A. Blanchard, M. Douspis, and M. Le Dour, in *Proceedings of the MPA-ESO Conference on Evolution of Large Scale Structure, Garching, 1998* (astro-ph/98103188); J. R. Bond and A. H. Jaffe, Philos. Trans. R. Soc. Lond. (astro-ph/9809043); C. H. Lineweaver, Science **284**, 1503 (1999); B. Ratra *et al.*, Astrophys. J. **517**, 549 (1999); M. Tegmark, Astrophys. J. **514**, L69 (1999).
- [3] S. Dodelson and L. Knox, Phys. Rev. Lett. **84**, 3523 (2000).
- [4] Others have also fit phenomenological models to the CMB power spectrum: D. Scott, M. White, and J. Silk (1995); Hancock and Rocha (1996).
- [5] G. Wilson *et al.*, Astrophys. J. **532**, 587 (2000).
- [6] K. Coble *et al.*, Astrophys. J. **519**, L5 (1999); K. Coble, Ph.D. thesis (astro-ph/9911419).
- [7] [TOCO97] E. Torbet *et al.*, Astrophys. J. **521**, L79 (1999); [TOCO98] A. Miller *et al.*, Astrophys. J. **524**, L1 (1999).
- [8] The Mobile Anisotropy Telescope (MAT), while situated on Cerro Toco, Chile, produced two data sets with the same instrument, calibrator, observing strategy, and region of sky. The data were taken by the same team and analyzed with the same software. TOCO97 and TOCO98 refer to two different seasons of the same experiment; we refer to them collectively as TOCO.
- [9] J. B. Peterson *et al.*, astro-ph/9910503.
- [10] J. C. Baker *et al.*, astro-ph/9904415.
- [11] Dicker *et al.*, astro-ph/9907118.
- [12] P. D. Mauskopf *et al.*, astro-ph/9911444.
- [13] For example, E. S. Cheng *et al.*, Astrophys. J. Lett. **488**, L59 (1997).
- [14] C. L. Bennett, A. J. Banday, K. M. Gorski, G. Hinshaw, P. D. Jackson, P. Keegstra, A. Kogut, G. F. Smoot, D. Wilkinson, and E. L. Wright, Astrophys. J. Lett. **464**, L1 (1996), and 4-year COBE/DMR references therein.
- [15] S. Burles, K. M. Nollett, J. W. Truran, and M. S. Turner, Phys. Rev. Lett. **82**, 4176 (1999).
- [16] J. R. Bond, A. H. Jaffe, and L. Knox, Astrophys. J. **533**, 19 (2000).
- [17] We modify the Gaussian by taking for $500 < l < 1000$, $\delta T_l^2 = 2000 \mu\text{K}^2$ and for $l > 1000$, $\delta T_l^2 = 0$. Assuming a Gaussian out to $l = 1000$ gives bad χ^2 values.
- [18] K. Ganga, B. Ratra, J. Gundersen, and N. Sugiyama, Astrophys. J. **484**, 517–522 (1997); see also astro-ph/9602141.
- [19] <http://flight.uchicago.edu/knox/radpack.html>
- [20] C. R. Contaldi, P. G. Ferreira, J. Magueijo, and K. M. Gorski, astro-ph/9910138 (1999).
- [21] For example, W. Hu and N. Sugiyama, Phys. Rev. D **51**, 2599 (1995); W. Hu and M. White, Astrophys. J. **471**, 30 (1996).
- [22] T. P. Viana and A. R. Liddle, Mon. Not. R. Astron. Soc. **281**, 323 (1996).
- [23] For example, J. Magueijo, A. Albrecht, P. Ferreira, and D. Coulson, Phys. Rev. D **54**, 3727 (1996).
- [24] J. Weller, R. A. Battye, and A. Albrecht, Phys. Rev. D **60**, 103520 (1999).
- [25] A. Albrecht, in Proceedings of the 2000 Moriond Conference (to be published).
- [26] W. Hu, Phys. Rev. D **59**, 021301 (1998); W. Hu and P. J. E. Peebles, astro-ph/9910222; N. Turok, Phys. Rev. Lett. **7**, 4138 (1996).
- [27] P. de Bernardis *et al.*, Nature (London) **404**, 955–959 (2000).